Knockdown of eukaryotic translation initiation factor 5A2 enhances the therapeutic efficiency of doxorubicin in hepatocellular carcinoma cells by triggering lethal autophagy

YUEXIAO TANG[1,2*], KE CHEN[3*], XIAORUI LUAN[1,2*], JINYAN ZHANG[1,2], RONGRONG LIU[4], XIAOXIAO ZHENG[2], SHANGZHI XIE[2], HAIPING KE[5], XIANNING ZHANG[1] and WEI CHEN[2]

[1]Department of Genetics, Zhejiang Provincial Key Laboratory of Genetic and Developmental Disorders, Institute of Cell Biology, Zhejiang University School of Medicine, Hangzhou, Zhejiang 310058; [2]Cancer Institute of Integrated Traditional Chinese and Western Medicine, Zhejiang Academy of Traditional Chinese Medicine, Tongde Hospital of Zhejiang Province, Hangzhou, Zhejiang 310012; [3]Department of General Surgery, Sir Run Run Shaw Hospital, Zhejiang University School of Medicine, Hangzhou, Zhejiang 310016; [4]Division of Hematology-Oncology, Children's Hospital, Zhejiang University School of Medicine, Hangzhou, Zhejiang 310003; [5]Department of Biology, Ningbo College of Health Sciences, Ningbo, Zhejiang 315100, P.R. China

Received June 23, 2020; Accepted October 13, 2020

DOI: 10.3892/ijo.2020.5143

Abstract. Hepatocellular carcinoma (HCC) is an invasive malignant neoplasm with a poor prognosis. The development of chemoresistance severely obstructs the chemotherapeutic efficiency of HCC treatment. Therefore, understanding the mechanisms of chemoresistance is important for improving the outcomes of patients with HCC. Eukaryotic translation initiation factor 5A2 (eIF5A2), which is considered to be an oncogene, has been reported to mediate chemoresistance in various types of cancer; however, its precise role in HCC remains unclear. Accumulating evidence has suggested that autophagy serves a dual role in cancer chemotherapy. The present study aimed to investigate the role of autophagy in eIF5A2-mediated doxorubicin resistance in HCC. High expression levels of eIF5A2 in human HCC tissues were observed by immunohistochemistry using a tissue microarray, which was consistent with the results of reverse transcription-quantitative PCR analysis in paired HCC and adjacent healthy tissues. HCC patient-derived tumor xenograft mouse model was used for the *in vivo* study, and knockdown of eIF5A2 effectively enhanced the efficacy of doxorubicin chemotherapy compared with that in the control group. Notably, eIF5A2 served as a repressor in regulating autophagy under chemotherapy. Silencing of eIF5A2 induced doxorubicin sensitivity in HCC cells by triggering lethal autophagy. In addition, 5-ethynyl-2'-deoxyuridine, lactate dehydrogenase release assay and calcein-AM/PI staining were used to determine the enhanced autophagic cell death induced by the silencing of eIF5A2 under doxorubicin treatment. Suppression of autophagy attenuated the sensitivity of HCC cells to doxorubicin induced by eIF5A2 silencing. The results also demonstrated that knockdown of the Beclin 1 gene, which is an autophagy regulator, reversed the enhanced autophagic cell death and doxorubicin sensitivity induced by eIF5A2 silencing. Taken together, these results suggested eIF5A2 may mediate the chemoresistance of HCC cells by suppressing autophagic cell death under chemotherapy through a Beclin 1-dependent pathway, and that eIF5A2 may be a novel potential therapeutic target for HCC treatment.

Correspondence to: Professor Xianning Zhang, Department of Genetics, Zhejiang Provincial Key Laboratory of Genetic and Developmental Disorders, Institute of Cell Biology, Zhejiang University School of Medicine, 866 Yuhangtang Road, Hangzhou, Zhejiang 310058, P.R. China
E-mail: zhangxianning@zju.edu.cn

Dr Wei Chen, Cancer Institute of Integrated Traditional Chinese and Western Medicine, Zhejiang Academy of Traditional Chinese Medicine, Tongde Hospital of Zhejiang province, 234 Gucui Road, Hangzhou, Zhejiang 310012, P.R. China
E-mail: wei_chen@zju.edu.cn

*Contributed equally

Key words: eukaryotic translation initiation factor 5A2, hepatocellular carcinoma, doxorubicin, chemotherapy, autophagic cell death

Introduction

Hepatocellular carcinoma (HCC) was the seventh leading type of cancer and the fourth leading cause of cancer-related death worldwide in 2017 (1,2). Liver cancer has a poor prognosis, with a ratio of mortality to incidence of 0.93 worldwide (2). Surgical resection, transplantation and percutaneous ablation are clinically available for the treatment of early-stage HCC (3,4). However, resistance to chemotherapy or radiotherapy has resulted in an absence of effective therapeutic options and a

poor prognosis, especially for patients with advanced HCC (5). Therefore, it is important to develop novel treatments or to reverse chemoresistance to improve the outcomes of patients with advanced HCC.

Eukaryotic translation initiation factor 5A (eIF5A or eIF5A1) is highly conserved throughout eukaryotic evolution and serves roles in mRNA translation, cellular proliferation, differentiation and inflammation (6). eIF5A and its homolog eIF5A2, a 17-kDa protein comprising 153 amino acids, are the only known proteins that contain a unique amino acid residue, hypusine, which is crucial for their function to maintain polyamine homeostasis (6,7). eIF5A2 is of particular interest since it is rare in the majority of normal tissues but abundant in the testes, parts of the brain and several types of malignant tissues including bladder and colorectal cancer as well as hepatocellular carcinoma (8,9). eIF5A2 has been proposed to be an oncogene, and overexpression of eIF5A2 has been demonstrated to promote cell aggressiveness in colorectal carcinoma (10), bladder cancer (11), melanoma (12) and gastric cancer (13). Furthermore, inhibition of eIF5A2 by N1-guanyl-1, 7-diaminoheptane, an inhibitor of deoxyhypusine synthase, has been demonstrated to enhance the chemotherapeutic effects of gemcitabine in pancreatic ductal adenocarcinoma cells (14) and that of doxorubicin in bladder cancer cells (11). Although a number of studies have been performed to understand the relationship between eIF5A2 and chemosensitivity (11,14), the mechanism underlying eIF5A2 and chemosensitivity in HCC remains unclear.

Autophagy, a lysosomal degradation pathway for providing energy and macromolecular precursors (15), has also been implicated in the development of chemoresistance. When cells encounter environmental stressors, such as nutrient starvation and pathogen infection, autophagy is induced to digest and recycle cellular proteins and organelles to sustain cellular metabolism, or to eliminate pathogens and apoptotic cells (16,17). Autophagy is also coordinated with the ubiquitin-proteasome system to remove polyubiquitinated and aggregated proteins (18). Therefore, autophagy may promote cell survival and contribute to chemoresistance. A number of studies have demonstrated that inhibition of autophagy overcomes chemoresistance in prostate cancer, leukemia and bladder cancer (19-21). The induction of autophagy has also been reported to cause a form of programmed cell death termed autophagic cell death (22-24). Furthermore, Segala *et al* (25) have reported that dendrogenin A, a cholesterol metabolite, directly controls a nuclear receptor to trigger lethal autophagy in melanoma. Autophagy has been identified as a cytoprotective mechanism in gastric carcinoma, leukemia and squamous cell carcinoma (26-28). In addition, autophagy serves a cytocidal role in breast and colorectal cancer (29,30). However, the role of autophagy in the chemoresistance or chemosensitivity in HCC remains controversial.

The present study aimed to determine the potential roles of eIF5A2 in doxorubicin sensitivity and to investigate the effects of autophagy during this process.

Materials and methods

Ethics statement. The present study was approved by the Research Ethics Committee of the Second Affiliated Hospital of Zhejiang University School of Medicine (approval no. 2018-238; Hangzhou, China). All samples were anonymously coded in accordance with local ethical guidelines (based on the Declaration of Helsinki), and written informed consent was obtained from all patients. All animals used received appropriate care according to the Institutional Animal Care and Use Committee at the Second Affiliated Hospital of Zhejiang University School of Medicine (approval no. 2018-311). All efforts were made to minimize animal suffering.

Cell lines and culture. The human hepatocellular carcinoma cell lines SNU449, SNU387 and Huh7 were purchased from the Cell Bank of Type Culture Collection of Chinese Academy of Sciences, Shanghai Institute of Cell Biology, Chinese Academy of Sciences. SNU449 and SNU387 cells were cultured in RPMI-1640 medium (Gibco; Thermo Fisher Scientific, Inc.). Huh7 cells were cultured in DMEM (Gibco; Thermo Fisher Scientific, Inc.). All culture media were supplemented with 10% heat-inactivated fetal bovine serum (FBS; Gibco; Thermo Fisher Scientific, Inc.), 100 U/ml penicillin and 100 mg/ml streptomycin, and all cells were maintained at 37˚C in a humidified incubator with 5% CO_2.

Antibodies and reagents. Anti-LC3B (1:1,000; cat. no. 3868S), SQSTM1/p62 (1:1,000; cat. no. 8025S), Beclin 1 (1:1,000, cat. no. 3495P), HRP-conjugated anti-mouse IgG (1:2,000; cat. no. 7076S) and HRP-conjugated anti-rabbit IgG (1:2,000; cat. no. 7074S) antibodies were purchased from Cell Signaling Technology, Inc. The anti-eIF5A2 (1:1,000; cat. no. ab126735) and anti-KI67 (1:200; cat. no. ab16667) antibodies were obtained from Abcam, and the anti-β-actin (1:1,000; cat. no. 66009-1-ig) antibody was from ProteinTech Group, Inc..

The eIF5A2 small interfering RNA (siRNA) and negative control siRNA were synthesized by Shanghai GenePharma Co., Ltd. The PT3-EF1a-eIF5A2-flag and PT3-EF1a plasmids were purchased from Wuhan Yuling Biological Technology Co., Ltd. Cell Counting Kit-8 (CCK-8; cat. no. AD10) was obtained from Dojindo Molecular Technologies, Inc. The 5-ethynyl-2'-deoxyuridine (EdU) kit (cat. no. A10044) and Lipofectamine® 2000 Transfection Reagent (cat. no. 11668019) were purchased from Invitrogen; Thermo Fisher Scientific, Inc. The autophagy inhibitor chloroquine (CQ; cat. no. C6628) and the mTOR inhibitor rapamycin (Rapa; cat. no. V900930) were obtained from Sigma-Aldrich; Merck KGaA. Doxorubicin (cat. no. S1208) was purchased from Selleck Chemicals. Monomeric red fluorescent protein (mRFP)-green fluorescent protein (GFP)-LC3 adeno-associated virus (AAV) was obtained from Hanbio Biotechnology Co., Ltd. 2'-O-methoxyethyl (2'-Ome)- and 5'-cholesterol (5'-chol)-modified eIF5A2 siRNA was chemically synthesized by Guangzhou RiboBio Co., Ltd.

Survival analysis. The tissue microarray containing 90 paired HCC and adjacent tissues was obtained from Shanghai Xinchao Biological Technology Co. Ltd. (cat. no. HLiv-HCC180Sur-04). The clinicopathological information about patient age, sex, tumor stage and survival was provided by Shanghai Xinchao Biological Technology Co. Ltd. The follow-up period ranged between 1 and 6 years. Immunohistochemistry (IHC)

staining of eIF5A2 was performed as follows: The tissue microarray was incubated with 3% H_2O_2 for 10 min at room temperature, followed by antigen retrieval in Tris-EDTA buffer containing 0.05% Tween 20 (pH 9.0) in a water bath at 95-100˚C for 15 min, incubation with 10% FBS in PBS for 30 min at room temperature, and further incubation with an anti-eIF5A2 (1:100; cat. no. ab126735; Abcam) antibody at 4˚C overnight. The tissues were subsequently incubated with an HRP-conjugated goat anti-rabbit IgG secondary antibody (1:200; cat. no. ab205718; Abcam) at room temperature for 30 min, followed by incubation with DAB (cat. no. ab64238; Abcam) at room temperature for 1-2 min according to the manufacturer's instructions and counterstaining with hematoxylin. The stained tissues were dehydrated and stabilize with mounting medium (cat. no. ab64230; Abcam). Images (magnification, x200) were captured using AperioImageScope software 11.1.2.752 (Leica Biosystems), and 5-10 fields of view per sample were analyzed. IHC analysis of the paired HCC and adjacent tissues in the microarray was used to evaluate eIF5A2 staining intensity and relative expression levels in tumors and adjacent tissues. Images (magnification, x200) were captured using Aperio ImageScope software 11.1.2.752 (Leica Biosystems), and 5-10 fields of view per sample were analyzed. The tissue scoring was confirmed by two independent pathologists who were blinded to the grouping. eIF5A2 staining score was based on staining intensity as follows: 0, none; 1, equivocal/uninterpretable; 2, weak; and 3, intermediate-strong. The proportion score was based on expression rate as follows: 0, none; 1, 1-25%; 2, 26-50%; 3, 51-75%; and 4, 76-100%. A composite score was obtained by multiplying the intensity score by the proportion score. A composite score <4 was considered low expression, and a score ≥4 was considered high expression. Long-term follow-up was obtained through tumor registries and telephone interviews. The survival curve was drawn by Kaplan-Meier method, and the difference was evaluated by log-rank test.

Patient samples. A total of 30 paired tumor and adjacent tissues (≥3 cm from the tumor margin) were collected from patients with HCC (mean age, 56 years; range, 38-78 years; 21 male and 9 female patients) undergoing surgery at the Second Affiliated Hospital of Zhejiang University School of Medicine between January and December 2018. The histological diagnosis of HCC was confirmed by two independent pathologists, and the samples were used for reverse transcription-quantitative PCR (RT-qPCR) and mouse model establishment.

RNA isolation. A total of 50-100 mg of HCC or adjacent tissue was homogenized in 1 ml TRIzol® reagent (Invitrogen; Thermo Fisher Scientific, Inc.) using a power homogenizer. For cells, 1 ml TRIzol® reagent was added to a culture dish to lyse the cells directly. The homogenized samples were incubated for 5 min at room temperature, and 0.2 ml chloroform per 1 ml of TRIzol reagent was added, followed by centrifugation of the samples at 12,000 x g for 15 min at 4˚C. Subsequently, the upper aqueous phase was transferred into fresh tubes, and 0.5 ml isopropyl alcohol was added, followed by centrifugation at 12,000 x g at 4˚C for 10 min. The supernatant was removed, and the RNA pellet was washed with 75% ethanol. Finally, the RNA was dissolved in DEPC-treated water at room temperature.

RT-qPCR. Following total RNA extraction, reverse transcription of mRNA was performed using a PrimeScript RT reagent kit with gDNA Eraser (Perfect Real Time) (Takara Bio, Inc.) according to the manufacturer's instructions. The mRNA levels of eIF5A2 and β-actin were quantified by qPCR using specific primers and a TB Green qPCR Master Mix (Takara Bio, Inc.) on a LightCycler® 480 II instrument (Roche Diagnostics). The thermocycling conditions were as follows: 95˚C for 30 sec; 40 cycles of 95˚C for 5 sec and 60˚C for 30 sec; and 50˚C for 30 sec. The primer sequences were as follows: eIF5A2 forward, 5'-TATGCAGTGCTCGGCCTTG-3' and reverse, 5'-TTGGAACATCCATGTTGTGAGTAGA-3'; and β-actin forward, 5'-TTCCAGCCTTCCTTCCTG-3' and reverse, 5'-CTTTGCGGATGTCCACGT-3'. Relative changes in the mRNA expression levels were analyzed using the $2^{-\Delta\Delta Cq}$ method (31). All experiments were carried out in triplicate and independently repeated three times.

Cell viability assay. Tumor cells were seeded into 96-well plates at 3,000 cells/well. Following adherence, the medium was replaced with medium containing 0, 0.125, 0.25, 0.5, 1, 2 or 5 μg/ml doxorubicin for 48 h at 37˚C. Subsequently, CCK-8 solution was added into the wells (1:1,000) for 2 h at 37˚C according to the manufacturer's instructions, and cell viability was determined at 450 nm using an Epoch Microplate Spectrophotometer (BioTek Instruments, Inc.). For the co-treatment with CQ or rapamycin, SNU449 cells were pretreated with 10 μM CQ (dissolved in ddH_2O) or 100 nM rapamycin (dissolved in DMSO) for 6 h and subsequently treated with eIF5A2 siRNA and doxorubicin.

In vivo analysis. A total of 20 male athymic BALB/c mice (age, 4-5 weeks; weight, 15-18 g) were obtained from the Model Animal Research Center of Nanjing University, Nanjing, China. The mice were housed in specific pathogen-free barrier facilities in a temperature-controlled room (24˚C) with a 12 h light-dark cycle and 35-40% relative humidity, and were permitted free access to food and drinking water. The body weight of each mouse was measured every 2 days. The mice were humanely sacrificed by cervical dislocation at the study endpoint.

Patient-derived xenograft (PDX) tumor tissues were used to establish the tumor model. Patient tumor in which eIF5A2 was detected by RT-qPCR was used to establishing the mouse model. The resected tumor was cut into 1 mm^3 fragments and inoculated subcutaneously into the flanks of the mice (one fragment per mouse). After 3 weeks, when the tumor volumes reached 50-100 mm^3, the mice were randomly divided into the following groups (n=5 mice/group): i) Control (saline); ii) doxorubicin; iii) eIF5A2 siRNA; and iv) eIF5A2 siRNA combined with doxorubicin. Saline and doxorubicin (2 mg/kg) were injected via the tail vein every 2 days. eIF5A2 siRNA (1 nmol/mouse) was administered via intratumoral injection every 2 days. To maintain the the stability of eIF5A2 siRNA *in vivo*, a 2'-OMe and 5'-chol modified siRNA was used. The 2'-OMe modification inhibits the ability of RNase H to cleave the bound sense RNA strand within the heteroduplex formed

between the nucleic acid and the target RNA (32), and the 5'-chol modification alters protein binding in serum, extending the circulation time, and facilitates direct cellular uptake (33). The body weights and tumor dimensions were measured every other day. The tumor volume was calculated using the modified ellipsoid formula: Volume=1/2 x (length x width^2). After 14 days, all mice were sacrificed, and the blood, liver, kidney and tumor tissues were harvested. The tissues were fixed with 4% formaldehyde for 48 h at 25˚C, and the liver, kidney and a part of each tumor were used for IHC. The remaining tumor tissues used for protein and mRNA expression analysis of eIF5A2 and autophagy-related genes.

IHC analysis and TUNEL assay. After the mice were sacrificed, the tumor tissues were dissected and fixed in formaldehyde. Following paraffin embedding, sectioning (5 μm), deparaffinization, incubation in 3% H_2O_2 for 10 min at room temperature, antigen retrieval by boiling in 0.01 M sodium citrate buffer (pH 6.0) for 15 min, the tissues were blocked with 10% FBS in PBS for 30 min at room temperature and stained with an anti-ki67 antibody (1:200) at 4˚C overnight. Subsequently, the sections were incubated with an HRP-conjugated goat anti-rabbit IgG secondary antibody (1:200) for 30 min at room temperature, incubated with DAB at for 1-2 min room temperature, counterstained with hematoxylin, dehydrated and stabilized with mounting medium (cat. no. ab64230; Abcam). For TUNEL assay, an *in situ* Cell Death Detection kit (Roche Molecular Diagnostics) was used to detect apoptosis according to the manufacturer's instructions following deparaffinization. The sections were counterstained with hematoxylin for 3 min at room temperature following dehydration and stabilizing with mounting medium. The slides were visualized under a Leica DM300 microscope (magnification, x200; Leica Microsystems GmbH), and 5-10 fields of view per sample were quantified using Leica Application Suite X software 3.0.0.15697 (Leica Microsystems GmbH).

Transfection. HCC cells (2x10^5) in the logarithmic phase of growth were seeded into 6-well plates and transfected with eIF5A2 siRNA (50 pmol), control siRNA (50 pmol), pT3-EF1a-eIF5A2-flag plasmid (2 μg) or pT3-EF1a plasmid (2 μg) when the cells reached a density of 50-60% using Lipofectamine® 2000 according to the manufacturer's instructions. The transfection medium (Opti-MEM; Gibco; Thermo Fisher Scientific, Inc.) was replaced with complete medium following 6-h incubation at 37˚C, and the cells were harvested after 48 h. The sequences of siRNAs were as follows: Negative control-homo sense, 5'-UUCUCCGAACGUGUCACGUTT-3' and anti-sense, 5'-ACGUGACACGUUCGGAGAATT-3'; eIF5A2-homo sense, 5'-GCAGACGAAAUUGAUUUCATT-3' and anti-sense, 5'-UGAAAUCAAUUUCGUCUGCTT-3'; and Beclin 1-homo sense, 5'-GUACCGACUUGUUCCCUAUTT-3' and anti-sense, 5'-AUAGGGAACAAGUCGGUACTT-3'.

Western blotting analysis. Cells were harvested in cell lysis buffer (Cell Signaling Technology, Inc.) containing protease inhibitors (Sigma-Aldrich; Merck KGaA) following treatment with eIF5A2 siRNA and doxorubicin for 48 h. The protein concentration was determined by BCA assay (Applygen Technologies, Inc.). A total of 10 μg protein was loaded per lane, separated by 15% SDS-PAGE and transferred to 0.45-μm polyvinylidene fluoride membranes (EMD Millipore). The membranes were blocked with TBS-Tween-20 (0.1% Tween-20) containing 0.5% BSA (cat. no. 4240GR100; NeoFroxx GmbH) and incubated with the aforementioned primary antibodies at 4˚C overnight. The membranes were washed with TBS-0.1% Tween-20 three times. Following incubation with anti-mouse IgG or anti-rabbit IgG secondary antibodies at 4˚C for 2 h, protein expression was detected by chemiluminescence with an EZ-ECL Chemiluminescence Detection Kit (Biological Industries).

EdU assay. Tumor cells were seeded in a 96-well plate at 3,000 cells/well and incubated with medium (RPMI-1640 medium for SNU449 and DMEM for Huh7) containing doxorubicin at the IC_{50} concentration for 48 h. Prior to fixation with 4% paraformaldehyde at 25˚C for 15 min, the cells were incubated with 10 μM EdU at 37˚C for 2 h. Next, membrane permeabilization for 15 min, EdU incubation for 30 min and Hoechst 33342 (Invitrogen; Thermo Fisher Scientific, Inc.) staining for 15 min were performed to stain EdU and the cell nuclei at 25˚C, respectively. Images were captured under na Olympus IX73 fluorescence microscope (magnification, x200; Olympus Corporation), and 5-10 fields of view per sample were analyzed.

Transmission electron microscopy (TEM) analysis. Following transfection with eIF5A2 siRNA for 48 h, SNU449 cells were fixed with glutaraldehyde at 4˚C for 16 h, followed by treatment with 1% osmic acid at 25˚C for >2 h, then rinsed with 0.1 M phosphate buffer, dehydrated sequentially in 50, 70 and 90% ethanol, 90% ethanol plus 90% acetone, 90 and 100% acetone for 15 min per step, and then embedded in Epon 812 embedding medium (Structure Probe, Inc.) according to the manufacturer's instructions. The samples were sectioned at 50-60 nm, stained with 3% uranyl acetate plus lead citrate, and images were captured using a transmission electron microscope (magnification, x25,000), and five fields of view per sample were analyzed.

Confocal microscopy. SNU449 cells were seeded into confocal dishes at 3x10^5 cells/well. Cells were treated with RPMI-1640 medium containing the mRFP-GFP-LC3 AAV at 37˚C for 6 h, incubated with eIF5A2 siRNA and doxorubicin at 37˚C for 48 h and fixed with 4% paraformaldehyde for 15 min at 25˚C. Images were captured using an Olympus IX81-FV1000 confocal microscope (magnification, x1,600; Olympus Corporation), and 5-10 fields of view of per sample were analyzed.

Apoptosis assay. Apoptosis was detected using Annexin V, FITC Apoptosis Detection kit (Dojindo Molecular Technologies, Inc.) After eIF5A2 siRNA and doxorubicin treatment for 48 h, 1x10^6 SNU449 cells were harvested by trypsinization and collected by centrifugation (300 x g at 4˚ for 3 min), resuspended in 100 μl binding buffer, stained with 5 μl annexin V-FITC and 5 μl propidium iodide (PI) at room temperature in the dark for 15 min according to the manufacturer's instructions, and then analyzed using a BD FACScanto II flow cytometer with BD FACSDiva software v8.0.1 (both from BD Biosciences).

Lactate dehydrogenase (LDH) release assay. HCC cells were seeded into a 96-well plate at 3,000 cells/well and administered eIF5A2 siRNA, eIF5A2 plasmid, CQ and rapamycin, alone or in combination at 37˚C for 48 h. The culture medium was collected by centrifugation at 300 x g for 3 min (4˚C) and transferred to a new 96-well plate, and the release of LDH was measured using a Cytotoxicity LDH Assay kit at 25˚C (Dojindo Molecular Technologies, Inc.) according to the manufacturer's instructions. LDH release was detected at 490 nm using an Epoch Microplate Spectrophotometer.

Cell death assay. SNU449 cells ($2x10^5$) in the logarithmic phase of growth were seeded in 6-well plates. After cells were administered eIF5A2 siRNA and Beclin 1 siRNA, alone or in combination at 37˚C for 48 h, cells were harvested by trypsinization and collected by centrifugation at 300 x g for 3 min, resuspended in trypan blue solution (T10282, Thermo Fisher Scientific, Inc.) and counted using a Countess II Automated Cell Counter with Countess II/II FL software v1.0.247 (both from Thermo Fisher Scientific, Inc.). The cell counter automatically quantified the trypan blue-positive dead cells and the trypan blue-negative living cells.

Calcein-AM/PI staining. SNU449 cells were seeded in a 96-well plate at 3,000 cells/well and administered eIF5A2 siRNA, eIF5A2 plasmid, CQ and rapamycin, alone or in combination at 37˚C for 48 h. The cells were then cultured with 1 μM calcein-AM and 3 μM PI (Cell Signaling Technology, Inc.) at 25˚C for 30 min. Subsequently, images were captured using an Olympus IX73 fluorescence microscope (magnification, x100), and five fields of view per were analyzed.

Statistical analysis. Data are presented as the mean ± SD from ≥3 independent replicates. Statistical analyses were performed using GraphPad Prism 7.0 (GraphPad Software, Inc.). Unpaired two-tailed Student's t-test was used to analyze differences between two groups, and one-way ANOVA with Tukey's post hoc test was used for multiple comparisons. $P<0.05$ was considered to indicate a statistically significant difference.

Results

eIF5A2 expression is negatively associated with the prognosis of patients with HCC. To investigate the role of eIF5A2 in HCC, a tissue microarray was used. Immunohistochemical staining of eIF5A2 protein in paired tumor and adjacent tissues from 90 patients with HCC revealed that the staining intensity of eIF5A2 was higher in tumor tissues compared with that in normal tissues (Fig. 1A and B). Based on the aberrant eIF5A2 expression, survival analysis revealed that high expression levels of eIF5A2 were associated with a shorter overall survival time of patients with HCC (Fig. 1C). In addition, eIF5A2 mRNA expression was detected in 30 pairs of tumors and adjacent tissues from patients with HCC. The tumor tissues exhibited higher expression levels of eIF5A2 compared with those in the adjacent normal tissues (Fig. 1D). These results suggested that eIF5A2 mRNA and protein expression levels were upregulated in HCC compared with those in normal tissues, and were associated with a poor prognosis.

To characterize the relationship between eIF5A2 and doxorubicin sensitivity, three HCC cell lines (SNU449, SNU387 and Huh7) were treated with 0.125-5 μg/ml doxorubicin. Sensitivity to doxorubicin was measured after 48-h treatment by CCK-8 assay. As demonstrated in Fig. 1E, among the tested cell lines, SNU449 was the most resistant to doxorubicin, followed by SNU387 and Huh7. Basal levels of eIF5A2 mRNA in the three cell lines were also assessed by RT-PCR (Fig. 1F). SNU449 had the highest expression of eIF5A2 while Huh7 had the lowest. Notably, the IC_{50} values for doxorubicin appeared to be associated with eIF5A2 expression (Fig. 1G). Collectively, these results suggested that eIF5A2 may serve as a biomarker of HCC and may be involved in doxorubicin sensitivity.

eIF5A2 silencing improves doxorubicin chemotherapy in vivo. To investigate the role of eIF5A2 in chemosensitivity, three specific siRNAs were designed to silence the expression of eIF5A2 (Fig. S1), and the most efficient one (sieIF5A2-3, further referred to as eIF5A2 siRNA) was selected for further experiments.

To further determine the effects of eIF5A2 on doxorubicin sensitivity, a patient-derived xenograft (PDX) mouse model was established. An HCC tumor with high expression levels of eIF5A2 (Fig. S2) was subcutaneously injected into mice. Following 14-day treatment, both doxorubicin administration and eIF5A2 siRNA injection were observed to inhibit tumor growth (Fig. 2A-C). Notably, co-administration of eIF5A2 siRNA markedly enhanced the therapeutic effects of doxorubicin on tumor suppression (Fig. 2A-C). Doxorubicin and eIF5A2 siRNA exhibited no significant effects on the mouse body weight (Fig. 2C). In addition, the combination of doxorubicin and eIF5A2 siRNA inhibited the proliferation of tumor cells (as demonstrated by IHC staining of ki67) and increased the apoptotic rate (analyzed by TUNEL assay) compared with those in the other three groups (Fig. 2D), suggesting that co-treatment with of eIF5A2 siRNA may improve the therapeutic efficiency of doxorubicin *in vivo*.

eIF5A2 is involved in regulating autophagy and chemosensitivity of HCC cells. To further determine the tumor-suppressing effects of eIF5A2 siRNA observed in the *in vivo* experiment, SNU449 and Huh7 cells were transfected with eIF5A2 siRNA or an eIF5A2-overexpressing plasmid, respectively, and doxorubicin sensitivity was evaluated using the CCK-8 assay. The results demonstrated that silencing of eIF5A2 enhanced the effects of doxorubicin on cell viability compared with those in the negative control group, whereas eIF5A2 upregulation impaired the cytotoxic effects of doxorubicin (Fig. 3A and B). In addition, doxorubicin treatment alone notably reduced the proliferation rate in SNU449 and Huh7 cells according to the results of the EdU incorporation assay, and transfection with eIF5A2 siRNA and doxorubicin treatment exhibited additive antiproliferative effects (Fig. 3C). By contrast, eIF5A2 overexpression promoted HCC cell proliferation of doxorubicin-treated cells. These results demonstrated that eIF5A2 silencing enhanced doxorubicin efficacy *in vitro*.

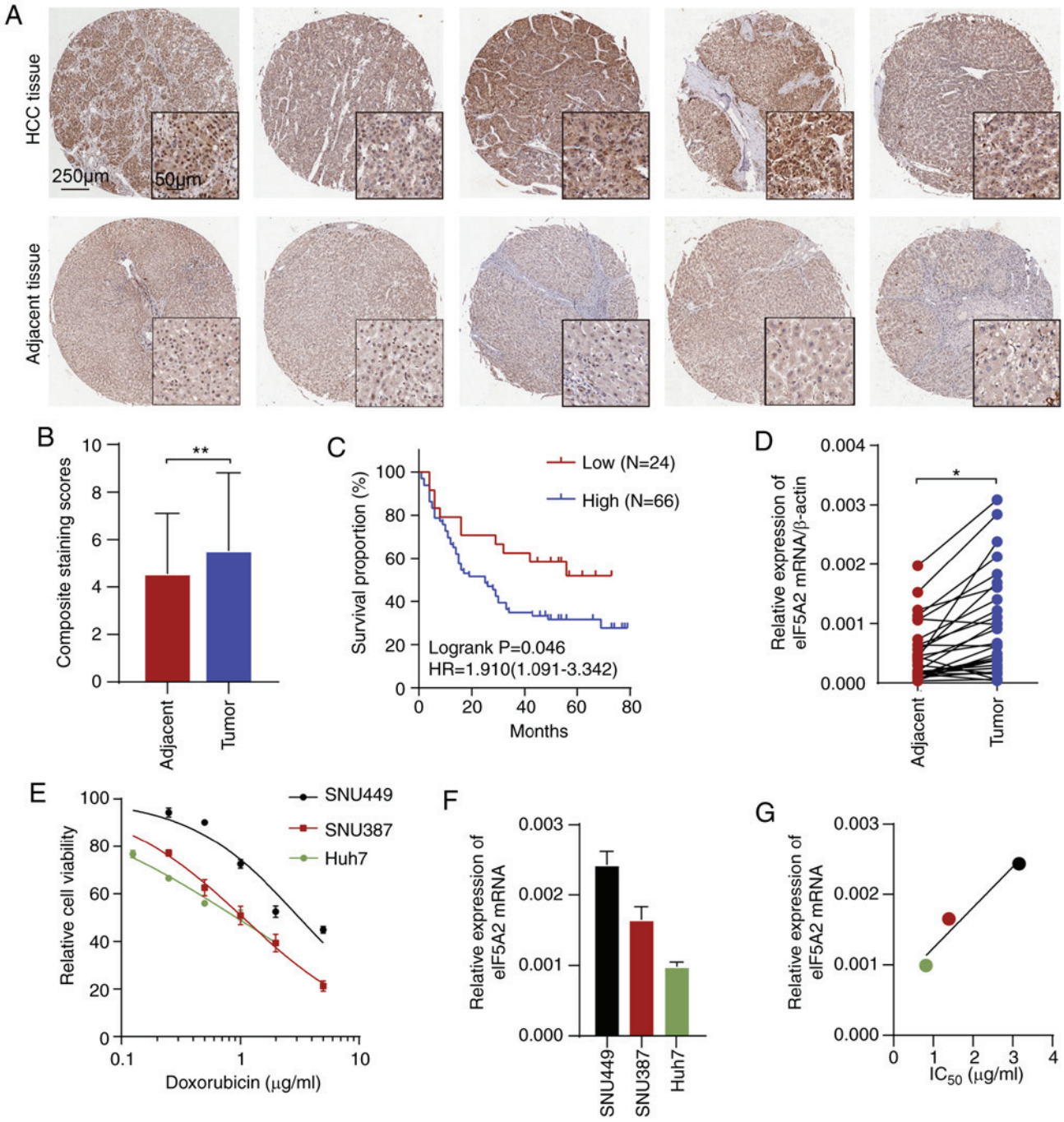

Figure 1. eIF5A2 expression is negatively associated with prognosis of patients with liver cancer. (A) Immunohistochemical staining of eIF5A2 protein in paired tumor and adjacent tissues. (B) Composite staining scores for eIF5A2 protein from 90 paired tumor and adjacent tissues. (C) Overall survival of 90 patients with HCC. (D) RT-qPCR analysis of eIF5A2 mRNA in paired tumor and adjacent tissues from patients with HCC (n=30). (E) HCC cells were treated with the indicated doses of doxorubicin for 48 h. Cell viability was determined by the Cell Counting Kit-8 assay. (F) RT-qPCR analysis of eIF5A2 mRNA in HCC cells. (G) Association between eIF5A2 expression and IC_{50} values of doxorubicin in HCC cells. *P<0.05 and **P<0.01. eIF5A2, eukaryotic translation initiation factor 5A2; HCC, hepatocellular carcinoma; RT-qPCR, reverse transcription-quantitative PCR.

eIF5A2 silencing also resulted in increased numbers of autophagosomes observed by TEM compared with those in the negative control group (Fig. 3D). In order to validate the appearance of autophagic characteristics, the cells were infected with an AAV expressing an mRFP-GFP-LC3 reporter protein for monitoring the autophagic flux (Fig. 3E). The results demonstrated that eIF5A2 knockdown induced an increase in the numbers of in autophagosomes and autolysosomes compared with those in the negative control group, suggesting that eIF5A2 siRNA-induced autophagy may be involved in doxorubicin sensitivity.

Silencing of eIF5A2 induces sensitivity to doxorubicin in HCC cells by triggering lethal autophagy. To determine the role of autophagy triggered by eIF5A2 siRNA in doxorubicin treatment, the autophagic flux of cells treated with doxorubicin and eIF5A2 siRNA alone or in combination was visualized. Knockdown efficiency of eIF5A2 siRNA was validated by

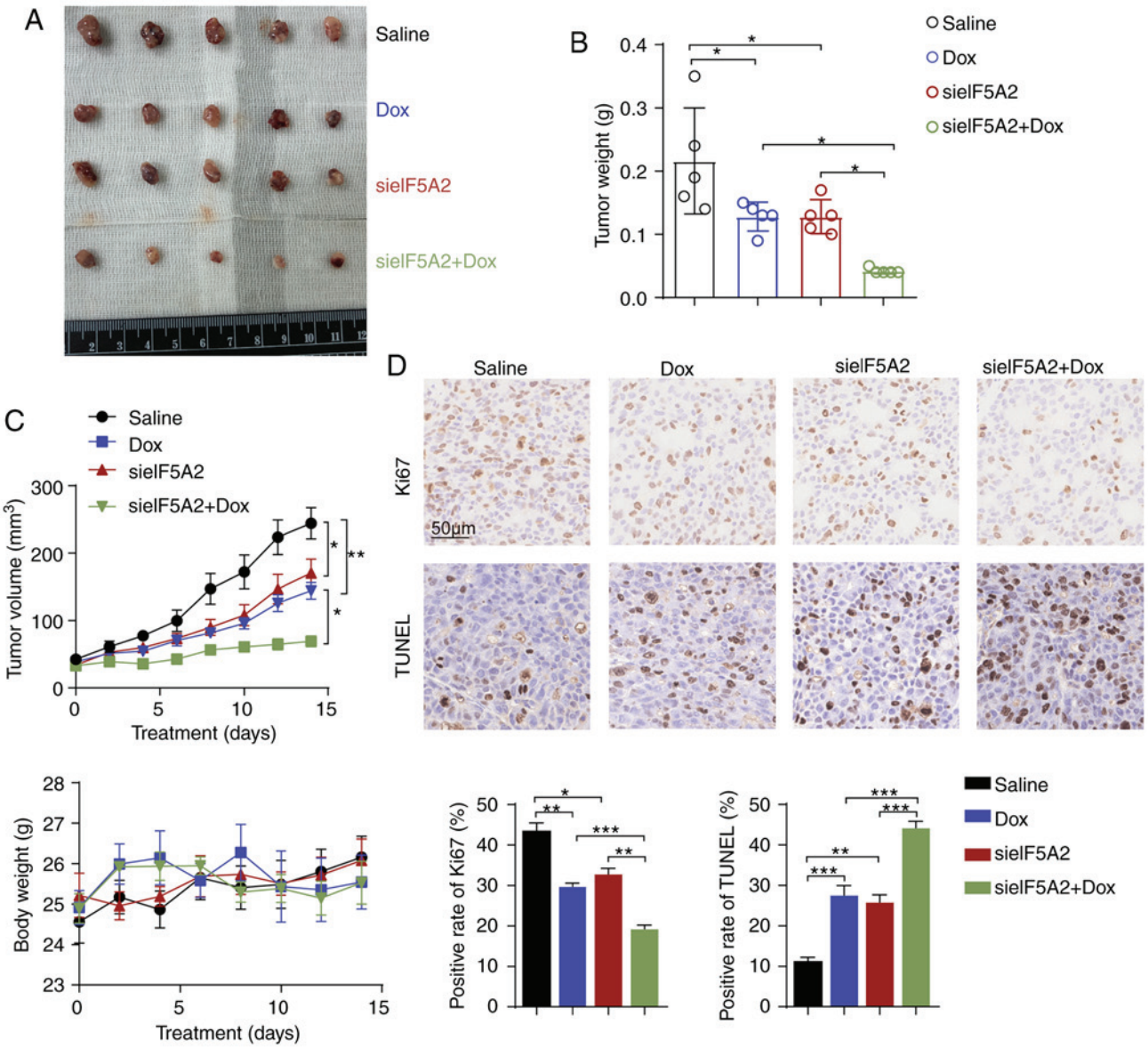

Figure 2. eIF5A2 silencing improves the efficacy of Dox chemotherapy *in vivo*. (A) Athymic nude mice (n=5 mice/group) engrafted with patient-derived xenograft tumor tissues were treated with saline, doxorubicin, sieIF5A2 or sieIF5A2 plus Dox. Xenograft tumors of hepatocellular carcinoma were imaged after 2-week treatment. (B) Tumor weight was assessed at the end of the experiments. (C) Tumor volumes and mouse body weights were monitored over time. (D) Immunohistochemical analysis of the expression of ki67 and TUNEL staining analysis in xenograft tumors dissected from mice of from the four experimental groups. The frequency of ki67 positive cells and TUNEL-positive cells was quantified. *P<0.05, **P<0.01 and ***P<0.001. eIF5A2, eukaryotic translation initiation factor 5A2; si, small interfering RNA; NC, negative control; Dox, doxorubicin.

western blotting (Fig. 4A). Doxorubicin treatment induced autophagic flux in SNU499 cells compared with that in the control group (Fig. 4B and C). In addition, combined eIF5A2 siRNA and doxorubicin treatment further reinforced the autophagic activity, with an increased number of autophagosomes compared with that observed in cells treated with doxorubicin alone (Fig. 4B and C). The protein expression levels of LC-3 I/II, Beclin 1 and p62 were evaluated by western blotting. The results demonstrated that eIF5A2 silencing markedly promoted the conversion of LC3I to LC3II, the formation of Beclin1 and the degradation of p62 compared with those in cells treated with doxorubicin alone (Fig. 4C), confirming that eIF5A2 siRNA promoted autophagy induced by doxorubicin. In addition, an increase of LDH release was observed in cells treated with eIF5A2 siRNA and doxorubicin compared with that in cells treated with doxorubicin alone, and eIF5A2 silencing accelerated doxorubicin-induced cell death (Fig. 4D). Notably, doxorubicin treatment alone activated apoptosis, but the apoptotic rate (early and late apoptosis) was only modestly further increased in the presence of eIF5A2 siRNA (Fig. 4E). These results suggested a limited additive effect between doxorubicin and eIF5A2 on apoptotic cell death.

eIF5A2 enhances HCC cell chemoresistance by suppressing autophagic cell death via a Beclin 1-dependent pathway. Since eIF5A2 siRNA and doxorubicin-induced autophagy was accompanied by cell death, we speculated that eIF5A2 knockdown may enhance doxorubicin-triggered autophagic cell death. To determine this, CQ, a pharmacological lysosomal inhibitor, was used to inhibit autophagy in SNU449 cells.

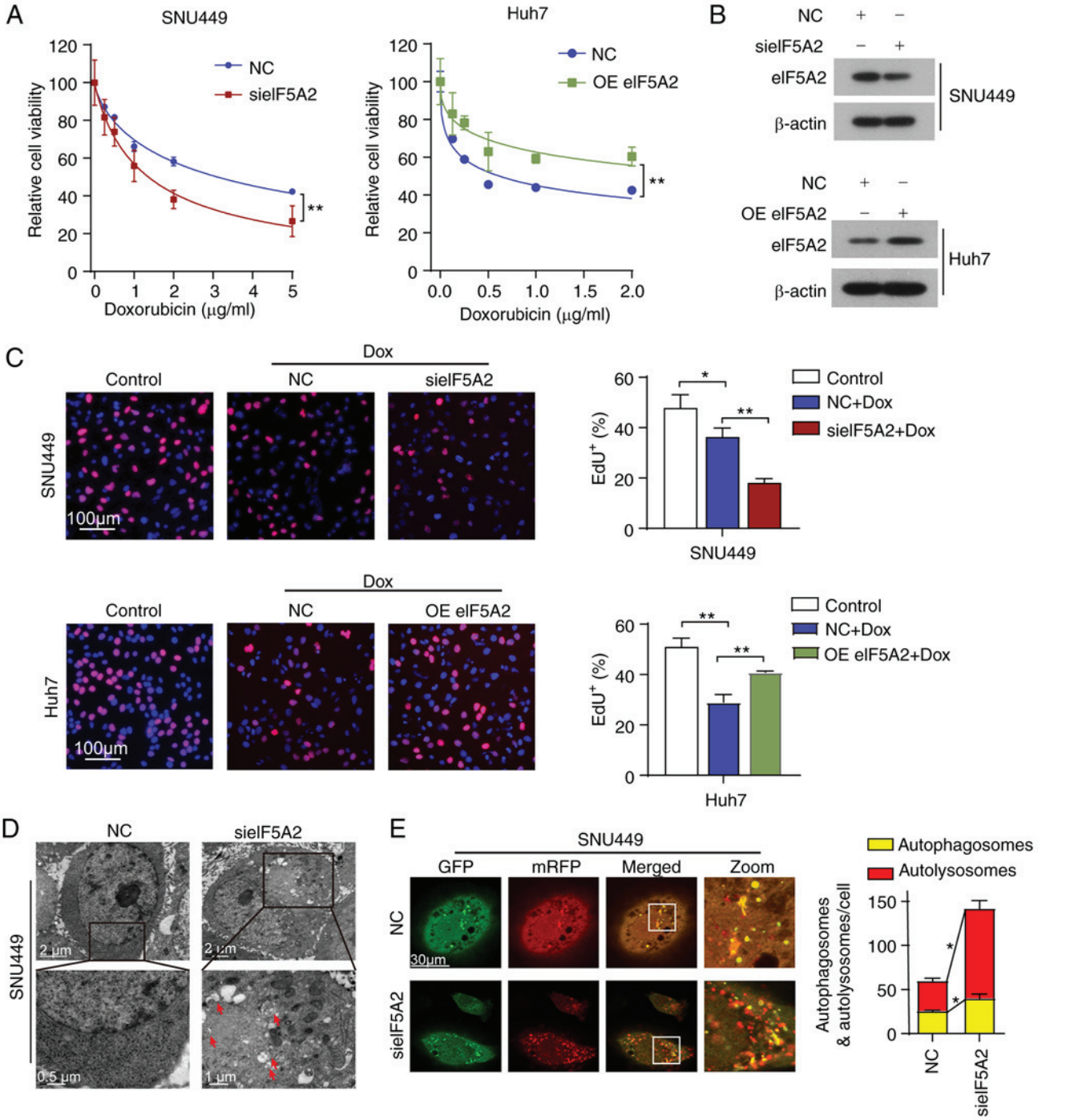

Figure 3. eIF5A2 is involved in the regulation of autophagy and chemosensitivity in HCC cells. (A) SNU449 cells were treated with indicated concentrations of Dox for 48 h following transfection with NC siRNA or sieIF5A2. Huh7 cells were treated with indicated concentrations of Dox for 48 h following transfection with an empty plasmid or OE eIF5A2. Cell viability was measured by the Cell Counting Kit-8 assay. (B) Western blotting analysis of eIF5A2 protein expression levels in HCC cells transfected with sieIF5A2 or OE eIF5A2. (C) HCC cells were treated with or without Dox for 48 h in the presence or absence of sieIF5A2 or OE eIF5A2. The cell proliferation rate was evaluated by EdU incorporation assay, and the frequency of EdU positive cells was quantified. (D) Autophagosomes were visualized in SNU449 cells treated with NC siRNA or sieIF5A2 by transmission electron microscopy. (E) SNU449 cells were infected with the mRFP-GFP-LC3 adenovirus and subsequently transfected with NC siRNA or sieIF5A2 and visualized by confocal microscopy. The numbers of GFP+/mRFP+-LC3 (yellow, autophagosomes) and GFP-/mRFP+-LC3 (red, autolysosomes) dots were counted and analyzed. *P<0.05 and **P<0.01. eIF5A2, eukaryotic translation initiation factor 5A2; EdU, 5-ethynyl-2'-deoxyuridine; HCC, hepatocellular carcinoma; siRNA, small interfering RNA; NC, negative control; sieIF5A2, siRNA against eIF5A2; OE, overexpression vector; mRFP, monomeric red fluorescent protein; GFP, green fluorescent protein; Dox, doxorubicin.

Notably, treatment with CQ partially reversed doxorubicin sensitivity and diminished eIF5A2 siRNA-mediated doxorubicin sensitivity (Fig. 5A and B). In addition, CQ attenuated the doxorubicin-induced increase in LDH release and cell death (Fig. 5C and D). CQ also inhibited the LDH release and cell death induced by the combination of eIF5A2 siRNA and doxorubicin. By contrast, Rapa, which is an autophagy activator, significantly decreased doxorubicin-induced cell death

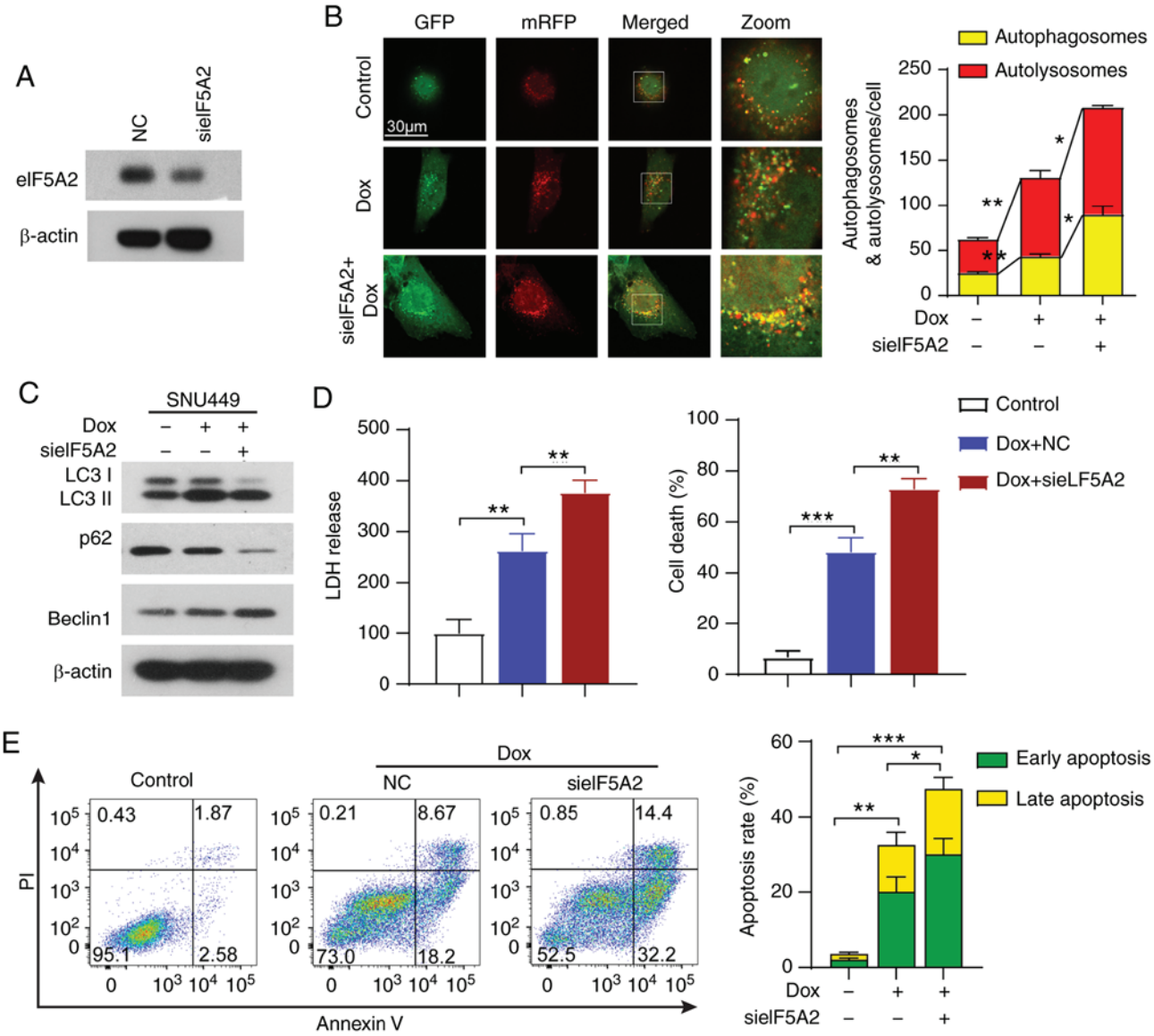

Figure 4. Silencing of eIF5A2 induces sensitivity to doxorubicin in HCC cells by triggering lethal autophagy. (A) Transfection efficiency of sieIF5A2 in SNU449 cells. (B) SNU449 cells were infected with the mRFP-GFP-LC3 adenovirus, treated with Dox and sieIF5A2 alone or in combination, and visualized by confocal microscopy. The numbers of $GFP^+/mRFP^+$-LC3 (yellow, autophagosomes) and $GFP^-/mRFP^+$-LC3 (red, autolysosomes) dots were counted and analyzed. (C) Western blotting analysis of LC3, p62 and Beclin 1 proteins in SNU449 cells treated with Dox and sieIF5A2 alone or in combination. (D) LDH release was detected in SNU449 cells following the indicated treatments. Cell death of SNU449 cells was detected using trypan blue staining. (E) Apoptotic rates in SNU449 cells were assessed by annexin V-VITC/PI apoptosis assay using flow cytometry following the indicated treatments. Early and late apoptotic rates were analyzed. $^*P<0.05$, $^{**}P<0.01$ and $^{***}P<0.001$. eIF5A2, eukaryotic translation initiation factor 5A2; si, small interfering RNA; NC, negative control; mRFP, monomeric red fluorescent protein; GFP, green fluorescent protein; Dox, doxorubicin; LDH, lactate dehydrogenase.

and reversed the cytoprotective effects of the overexpression of eIF5A2 (Fig. 5E-H). These results suggested that eIF5A2 siRNA may enhance doxorubicin sensitivity by inducing autophagic cell death in HCC cells.

To further investigate the underlying mechanisms, the protein levels of eIF5A2, LC-3 I/II, Beclin 1 and p62 in xenograft tumors were detected. Consistently with the results of the *in vitro* experiments, doxorubicin and eIF5A2 siRNA treatment increased the protein expression levels of LC3II and Beclin 1, but reduced the levels of p62 compared with those in the control group (Fig. 6A). Combination of doxorubicin and eIF5A2 siRNA induced higher LC3II and Beclin 1 and lower p62 protein expression levels compared with those observed following either therapy alone (Fig. 6A), indicating high levels autophagic activity in xenograft tumors under combined treatment. In addition, knockdown of Beclin 1 impaired the sensitivity of HCC cells to doxorubicin (Fig. 6B and C), and co-transfection with eIF5A2 siRNA did not restore the doxorubicin sensitivity of HCC cells following Beclin 1 knockdown (Fig. 6C). Similarly, knockdown of Beclin1 inhibited the combination treatment-induced LDH release and cell death (Fig. 6D and E). Taken together, these results demonstrated that the effects of eIF5A2 inhibition on autophagic cell death were mediated by Beclin 1.

Discussion

HCC is the third leading cause of cancer-related death worldwide (2). Multi-drug resistance diminishes the efficiency of

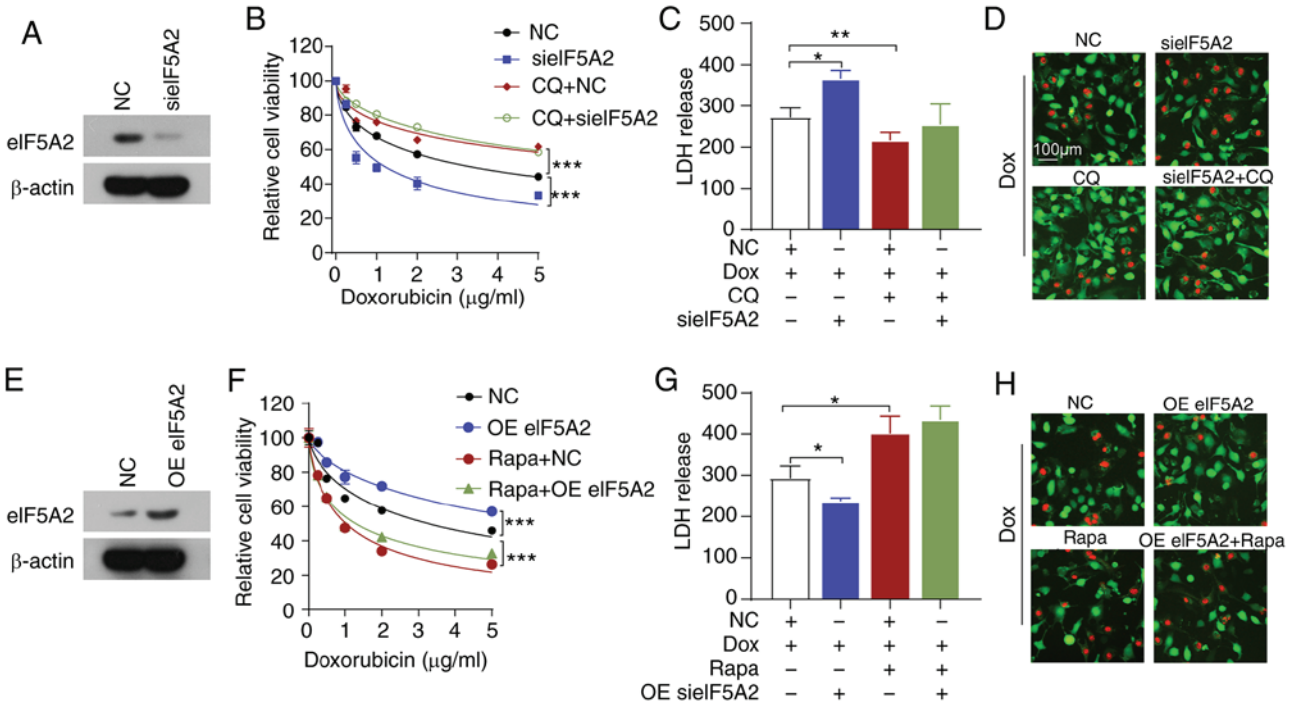

Figure 5. Combination of sieIF5A2 and Dox induces lethal autophagy. (A-D) SNU449 cells were treated with Dox, CQ and sieIF5A2 alone or in combination. (A) Transfection efficiency was assessed by western blotting. (B) Cell viability was assessed by CCK-8 assay. (C) LDH release was measured using an LDH assay. (D) Cell death was detected by Calcein-AM/PI staining. (E-H) SNU449 cells were treated with Dox, Rapa and OE eIF5A2 alone or in combination. (E) Transfection efficiency was assessed by western blotting. (F) Cell viability was assessed by CCK-8 assay. (G) LDH release was measured using an LDH assay. (H) Cell death was detected by Calcein-AM/PI staining. *P<0.05, **P<0.01 and ***P<0.001. eIF5A2, eukaryotic translation initiation factor 5A2; si, small interfering RNA; NC, negative control; CCK-8, Cell Counting Kit-8; LDH, lactate dehydrogenase; CQ, chloroquine; Rapa, rapamycin; OE, overexpression vector; Dox, doxorubicin.

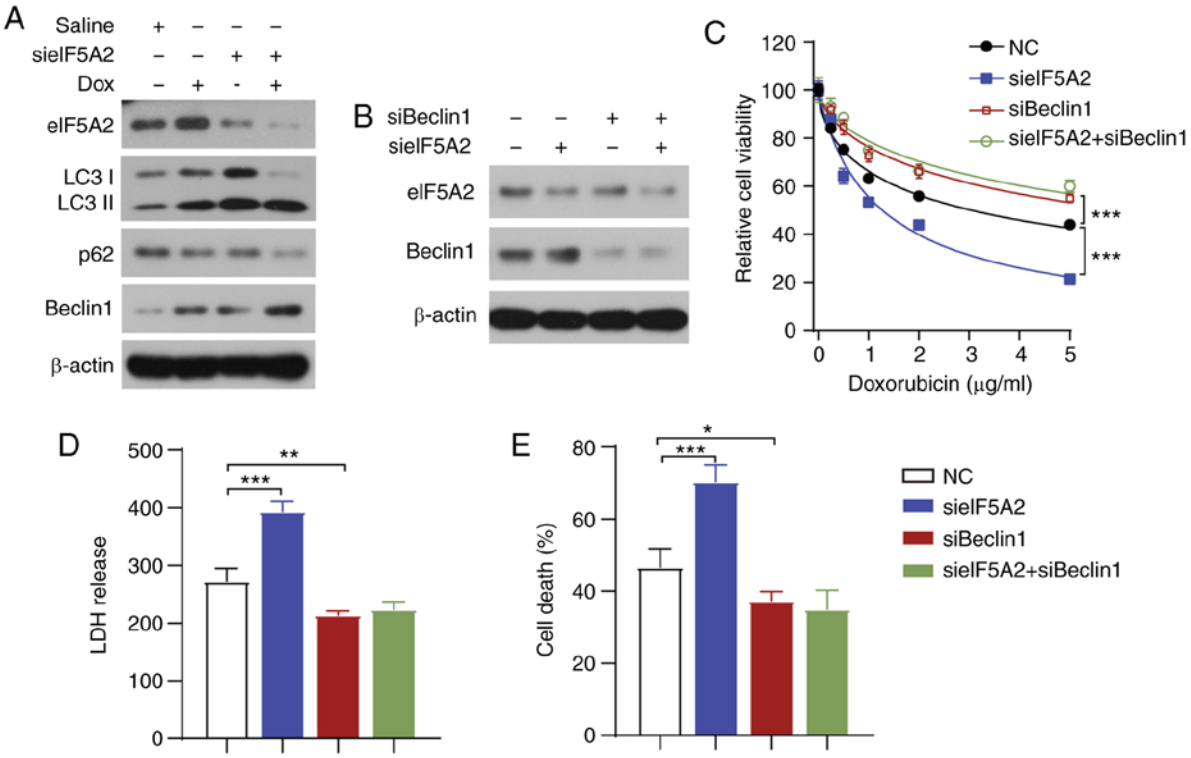

Figure 6. eIF5A2 knockdown triggers cell death via a Beclin 1-dependent pathway. (A) Western blotting analysis of eIF5A2, LC3, p62 and Beclin 1 protein expression levels in hepatocellular carcinoma xenograft tumors dissected from mice at the end of the *in vivo* experiment. (B-E) SNU449 cells were treated with the indicated concentrations of Dox with single or double knockdown of eIF5A2 and Beclin 1. (B) Transfection efficiency was assessed by western blotting. (C) Cell viability was assessed by Cell Counting Kit-8 assay. (D) LDH release was measured using an LDH assay. (E) Cell death was detected by trypan blue exclusion assay. *P<0.05, **P<0.01 and ***P<0.001. eIF5A2, eukaryotic translation initiation factor 5A2; Dox, doxorubicin; si, small interfering RNA; NC, negative control; LDH, lactate dehydrogenase.

therapeutic agents in HCC; therefore, developing new strategies to enhance chemotherapy efficiency is urgent. The results of the present study demonstrated that the expression levels of eIF5A2 were significantly upregulated in tumor tissues compared with those in adjacent normal tissues and were negatively associated with the overall survival of patients with HCC. In addition, eIF5A2 levels were positively associated with doxorubicin resistance in HCC cells, and eIF5A2 silencing enhanced the antitumor effects of doxorubicin *in vitro* and *in vivo*. Further experiments revealed that eIF5A2 siRNA improved the therapeutic efficiency of doxorubicin in HCC by triggering autophagic cell death through a Beclin 1-dependent pathway.

eIF5A2 is an oncogene highly expressed in several types of human cancer, including melanoma, gastric, breast and gallbladder cancer (11,12,34-36). Accumulating evidence suggests that eIF5A2 is involved in tumor initiation, growth, metastasis and chemoresistance (37-39). In particular, previous studies have demonstrated that inhibition or knockdown of eIF5A2 reverses chemoresistance in gastric and colorectal cancer, as well as in HCC (34,35,39-41). In addition, Yang *et al* (42) have reported that eIF5A2 overexpression significantly enhanced the resistance of esophageal squamous cell carcinoma cells to 5-fluorouracil by inhibiting apoptosis. Consistent with these, the present study demonstrated that eIF5A2 was upregulated in HCC, and eIF5A2 silencing enhanced the tumor-suppressing effects of doxorubicin both *in vivo* and *in vitro*. The results of the present study also demonstrated that overexpression of eIF5A2 induced resistance to doxorubicin. These results suggested a crucial role of eIF5A2 in the development of chemoresistance in HCC.

Autophagy is a double-edged sword, as the modulation (either activation or inhibition) of autophagy has been demonstrated to at least partly overcome or reverse doxorubicin resistance in breast cancer, hepatocellular carcinoma and osteosarcoma (43). Previous studies have suggested that autophagy serves as a pro-survival role, resulting in acquired resistance to chemotherapeutic agents in cancer (16,44). However, the cell death-promoting effects of autophagy have also been reported (25,45). For example, Tai *et al* (46) have demonstrated that sorafenib inhibits tumor growth by inducing autophagic cell death in HCC. Similarly, Wu *et al* (47) have reported that blocking β2 adrenoreceptor signaling enhanced sorafenib-induced autophagy and improved the antitumor effects of sorafenib in HCC. The results of the present study demonstrated that doxorubicin treatment induced autophagy, and that blocking autophagy with CQ impaired doxorubicin efficiency, suggesting that doxorubicin caused autophagic cell death. Notably, the results of further experiments revealed that knockdown of eIF5A2 enhanced cell death by triggering sustained lethal autophagy induced by doxorubicin. Beclin 1 was the first autophagy-related protein identified in mammals and serves a central role in autophagy (48). Beclin 1 constitutes a molecular platform for the regulation of autophagosome formation and maturation by forming distinct PI3K complexes together with the core lipid kinase VPS34 and the regulatory component VPS15 (49). Therefore, Beclin 1 can be used as a marker to monitor autophagy (17). The results of the present study demonstrated that knockdown of Beclin 1 reversed the eIF5A2 siRNA-mediated increase in doxorubicin sensitivity, revealing a potential mechanism of eIF5A2 siRNA-enhanced doxorubicin lethality.

In conclusion, the present study described the roles of eIF5A2 and autophagy in doxorubicin treatment of HCC. The results of the present study suggested that knockdown of eIF5A2 restored the sensitivity of HCC cells to doxorubicin by triggering lethal autophagy via a Beclin1-dependent signaling pathway. These results provide an potential target of HCC chemoresistance.

Acknowledgements

Not applicable.

Funding

This study was supported by the Zhejiang Provincial Ten Thousand Plan for Young Top Talents (2018), the Innovative Talents Training Project of Zhejiang Health Bureau (2018), the Key Project Co-constructed by the Zhejiang Province and Ministry (grant no. WKJ-ZJ-1916), the National High Technology Research and Development Program of China (grant no. SS2014AA020533), the Zhejiang Provincial Natural Science Foundation of China (grant no. LQ13H160006) and the Natural Science Foundation of China (grant nos. 81302071 and 81673809).

Availability of data and materials

The datasets generated and/or analyzed in the current study are available from the corresponding author on reasonable request.

Authors' contributions

YXT, WC and XNZ designed the study. KC and XRL performed the *in vitro* experiments and analyzed the data. JYZ, RRL, XXZ and SZX performed the *in vivo* experiments. HPK provided the experimental tools and analyzed the *in vivo* results. YXT, KC and XRL wrote the manuscript. WC and XNZ revised the manuscript. All authors read and approved the final manuscript.

Ethics approval and consent to participate

The present study was approved by the Ethics Committee of the Second Affiliated Hospital of Zhejiang University School of Medicine (Hangzhou, China), and written informed consent was obtained from all participants. All experimental procedures on animals were approved by the Institutional Animal Care and Use Committee at Zhejiang University School of Medicine.

Patient consent for publication

Not applicable.

Competing interests

The authors declare that they have no competing interests.

References

1. Global Burden of Disease Cancer Collaboration; Fitzmaurice C, Abate D, Abbasi N, Abbastabar H, Abd-Allah F, Abdel-Rahman O, Abdelalim A, Abdoli A, Abdollahpour I, *et al*: Global, regional, and national cancer incidence, mortality, years of life lost, years lived with disability, and disability-adjusted life-years for 29 cancer groups, 1990 to 2017: A systematic analysis for the global burden of disease study. JAMA Oncol 5: 1749-1768, 2019.
2. Bray F, Ferlay J, Soerjomataram I, Siegel RL, Torre LA and Jemal A: Global cancer statistics 2018: GLOBOCAN estimates of incidence and mortality worldwide for 36 cancers in 185 countries. CA Cancer J Clin 68: 394-424, 2018.
3. Ma MC, Chen YY, Li SH, Cheng YF, Wang CC, Chiu TJ, Pei SN, Liu CT, Huang TL, Huang CH, *et al*: Intra-arterial chemotherapy with doxorubicin and cisplatin is effective for advanced hepatocellular cell carcinoma. ScientificWorldJournal 2014: 160138, 2014.
4. Bruix J, Reig M and Sherman M: Evidence-based diagnosis, staging, and treatment of patients with hepatocellular carcinoma. Gastroenterology 150: 835-853, 2016.
5. Ma S, Lee TK, Zheng BJ, Chan KW and Guan XY: CD133+ HCC cancer stem cells confer chemoresistance by preferential expression of the Akt/PKB survival pathway. Oncogene 27: 1749-1758, 2008.
6. Schuller AP, Wu CC, Dever TE, Buskirk AR and Green R: eIF5A functions globally in translation elongation and termination. Mol Cell 66: 194-205 e5, 2017.
7. Taylor CA, Zheng Q, Liu Z and Thompson JE: Role of p38 and JNK MAPK signaling pathways and tumor suppressor p53 on induction of apoptosis in response to Ad-eIF5A1 in A549 lung cancer cells. Mol Cancer 12: 35, 2013.
8. Mathews MB and Hershey JW: The translation factor eIF5A and human cancer. Biochim Biophys Acta 1849: 836-844, 2015.
9. Caraglia M, Park MH, Wolff EC, Marra M and Abbruzzese A: eIF5A isoforms and cancer: Two brothers for two functions? Amino Acids 44: 103-109, 2013.
10. Zhu W, Cai MY, Tong ZT, Dong SS, Mai SJ, Liao YJ, Bian XW, Lin MC, Kung HF, Zeng YX, *et al*: Overexpression of EIF5A2 promotes colorectal carcinoma cell aggressiveness by upregulating MTA1 through C-myc to induce epithelial-mesenchymaltransition. Gut 61: 562-575, 2012.
11. Yang J, Yu H, Shen M, Wei W, Xia L and Zhao P: N1-guanyl-1,7-diaminoheptane sensitizes bladder cancer cells to doxorubicin by preventing epithelial-mesenchymal transition through inhibition of eukaryotic translation initiation factor 5A2 activation. Cancer Sci 105: 219-227, 2014.
12. Khosravi S, Wong RP, Ardekani GS, Zhang G, Martinka M, Ong CJ and Li G: Role of EIF5A2, a downstream target of Akt, in promoting melanoma cell invasion. Br J Cancer 110: 399-408, 2014
13. Meng QB, Kang WM, Yu JC, Liu YQ, Ma ZQ, Zhou L, Cui QC and Zhou WX: Overexpression of eukaryotic translation initiation factor 5A2 (EIF5A2) correlates with cell aggressiveness and poor survival in gastric cancer. PLoS One 10: e0119229, 2015.
14. Yao M, Hong Y, Liu Y, Chen W and Wang W: N1-guanyl-1, 7-diaminoheptane enhances the sensitivity of pancreatic ductal adenocarcinoma cells to gemcitabine via the inhibition of eukaryotic translation initiation factor 5A2. Exp Ther Med 14: 2101-2107, 2017.
15. Levy JMM, Towers CG and Thorburn A: Targeting autophagy in cancer. Nat Rev Cancer 17: 528-542, 2017.
16. Ding ZB, Hui B, Shi YH, Zhou J, Peng YF, Gu CY, Yang H, Shi GM, Ke AW, Wang XY, *et al*: Autophagy activation in hepatocellular carcinoma contributes to the tolerance of oxaliplatin via reactive oxygen species modulation. Clin Cancer Res 17: 6229-6238, 2011.
17. Hayat MA: Autophagy: Cancer, other pathologies, inflammation, immunity, infection, and aging. Vol 1. 1st edition. Elsevier Academic Press, 2016.
18. Pohl C and Dikic I: Cellular quality control by the ubiquitin-proteasome system and autophagy. Science 366: 818-822, 2019.
19. Hu F, Zhao Y, Yu Y, Fang JM, Cui R, Liu ZQ, Guo XL and Xu Q: Docetaxel-mediated autophagy promotes chemoresistance in castration-resistant prostate cancer cells by inhibiting STAT3. Cancer Lett 416: 24-30, 2018.
20. Piya S, Andreeff M and Borthakur G: Targeting autophagy to overcome chemoresistance in acute myleogenous leukemia. Autophagy 13: 214-215, 2017.
21. Zeng Q, Liu J, Cao P, Li J, Liu X, Fan X, Liu L, Cheng Y, Xiong W, Li J, *et al*: Inhibition of REDD1 sensitizes bladder urothelial carcinoma to paclitaxel by inhibiting autophagy. Clin Cancer Res 24: 445-459, 2018.
22. Fulda S and Kogel D: Cell death by autophagy: Emerging molecular mechanisms and implications for cancer therapy. Oncogene 34: 5105-5113, 2015.
23. Wang H, Lu Q, Cheng S, Wang X and Zhang H: Autophagy activity contributes to programmed cell death in Caenorhabditis elegans. Autophagy 9: 1975-1982, 2013.
24. Wang X, Wei S, Zhao Y, Shi C, Liu P, Zhang C, Lei Y, Zhang B, Bai B, Huang Y and Zhang H: Anti-proliferation of breast cancer cells with itraconazole: Hedgehog pathway inhibition induces apoptosis and autophagic cell death. Cancer Lett 385: 128-136, 2017.
25. Segala G, David M, de Medina P, Poirot MC, Serhan N, Vergez F, Mougel A, Saland E, Carayon K, Leignadier J, *et al*: Dendrogenin A drives LXR to trigger lethal autophagy in cancers. Nat Commun 8: 1903, 2017.
26. Masui A, Hamada M, Kameyama H, Wakabayashi K, Takasu A, Imai T, Iwai S and Yura Y: Autophagy as a survival mechanism for squamous cell carcinoma cells in endonuclease G-mediated apoptosis. PLoS One 11: e0162786, 2016.
27. Kun Z, Hanqing G, Hailing T, Yuan Y, Jun Z, Lingxia Z, Kun H and Xin Z: Gastrin enhances autophagy and promotes gastric carcinoma proliferation via inducing AMPKα. Oncol Res 25: 1399-1407, 2017.
28. Altman JK, Szilard A, Goussetis DJ, Sassano A, Colamonici M, Gounaris E, Frankfurt O, Giles FJ, Eklund EA, Beauchamp EM and Platanias LC: Autophagy is a survival mechanism of acute myelogenous leukemia precursors during dual mTORC2/mTORC1 targeting. Clin Cancer Res 20: 2400-2409, 2014.
29. Wu Q, Deng J, Fan D, Duan Z, Zhu C, Fu R and Wang S: Ginsenoside Rh4 induces apoptosis and autophagic cell death through activation of the ROS/JNK/p53 pathway in colorectal cancer cells. Biochem Pharmacol 148: 64-74, 2018.
30. Sun D, Zhu L, Zhao Y, Jiang Y, Chen L, Yu Y and Ouyang L: Fluoxetine induces autophagic cell death via eEF2K-AMPK-mTOR-ULK complex axis in triple negative breast cancer. Cell Prolif 51: e12402, 2018.
31. Livak KJ and Schmittgen TD: Analysis of relative gene expression data using real-time quantitative PCR and the 2(-Delta Delta C(T)) method. Methods 25: 402-408, 2001.
32. Yamakawa K, Nakano-Narusawa Y, Hashimoto N, Yokohira M and Matsuda Y: Development and clinical trials of nucleic acid medicines for pancreatic cancer treatment. Int J Mol Sci 20: 4224, 2019.
33. Behlke MA: Chemical modification of siRNAs for in vivo use. Oligonucleotides 18: 305-319, 2008.
34. Liu Y, Du F, Chen W, Yao M, Lv K and Fu P: EIF5A2 is a novel chemoresistance gene in breast cancer. Breast Cancer 22: 602-607, 2015.
35. Sun J, Xu Z, Lv H, Wang Y, Wang L, Ni Y, Wang X, Hu C, Chen S, Teng F, *et al*: eIF5A2 regulates the resistance of gastric cancer cells to cisplatin via induction of EMT. Am J Transl Res 10: 4269-4279, 2018.
36. Zheng X, Gao L, Wang BT, Shen P, Yuan XF, Zhang LQ, Yang L, Zhang DP, Zhang Q and Wang XM: Overexpression of EIF5A2 is associated with poor survival and aggressive tumor biology in gallbladder cancer. Histol Histopathol 35: 579-587, 2020.
37. Huang PY, Zeng TT, Ban X, Li MQ, Zhang BZ, Zhu YH, Hua WF, Mai HQ, Zhang L, Guan XY and Li Y: Expression of EIF5A2 associates with poor survival of nasopharyngeal carcinoma patients treated with induction chemotherapy. BMC Cancer 16: 669, 2016.
38. Li Y, Fu L, Li JB, Qin Y, Zeng TT, Zhou J, Zeng ZL, Chen J, Cao TT, Ban X, *et al*: Increased expression of EIF5A2, via hypoxia or gene amplification, contributes to metastasis and angiogenesis of esophageal squamous cell carcinoma. Gastroenterology 146: 1701-1713.e9, 2014.
39. Xue F, Liu Y, Chu H, Wen Y, Yan L, Tang Q, Xiao E, Zhang D and Zhang H: eIF5A2 is an alternative pathway for cell proliferation in cetuximab-treated epithelial hepatocellular carcinoma. Am J Transl Res 8: 4670-4681, 2016.
40. Fang L, Gao L, Xie L and Xiao G: Eukaryotic translation initiation factor 5A-2 involves in doxorubicin-induced epithelial-mesenchymal transition in oral squamous cell carcinoma cells. J Cancer 9: 3479-3488, 2018.

41. Bao Y, Lu Y, Wang X, Feng W, Sun X, Guo H, Tang C, Zhang X, Shi Q and Yu H: Eukaryotic translation initiation factor 5A2 (eIF5A2) regulates chemoresistance in colorectal cancer through epithelial mesenchymal transition. Cancer Cell Int 15: 109, 2015.
42. Yang H, Li XD, Zhou Y, Ban X, Zeng TT, Li L, Zhang BZ, Yun J, Xie D, Guan XY and Li Y: Stemness and chemotherapeutic drug resistance induced by EIF5A2 overexpression in esophageal squamous cell carcinoma. Oncotarget 6: 26079-26089, 2015.
43. Chen C, Lu L, Yan S, Yi H, Yao H, Wu D, He G, Tao X and Deng X: Autophagy and doxorubicin resistance in cancer. Anticancer Drugs 29: 1-9, 2018.
44. Li L, Wang Y, Jiao L, Lin C, Lu C, Zhang K, Hu C, Ye J, Zhang D, Wu H, *et al*: Protective autophagy decreases osimertinib cytotoxicity through regulation of stem cell-like properties in lung cancer. Cancer Lett 452: 191-202, 2019.
45. Dai CH, Shu Y, Chen P, Wu JN, Zhu LH, Yuan RX, Long WG, Zhu YM and Li J: YM155 sensitizes non-small cell lung cancer cells to EGFR-tyrosine kinase inhibitors through the mechanism of autophagy induction. Biochim Biophys Acta Mol Basis Dis 1864: 3786-3798, 2018.
46. Tai WT, Shiau CW, Chen HL, Liu CY, Lin CS, Cheng AL, Chen PJ and Chen KF: Mcl-1-dependent activation of Beclin 1 mediates autophagic cell death induced by sorafenib and SC-59 in hepatocellular carcinoma cells. Cell Death Dis 4: e485, 2013.
47. Wu FQ, Fang T, Yu LX, Lv GS, Lv HW, Liang D, Li T, Wang CZ, Tan YX, Ding J, *et al*: ADRB2 signaling promotes HCC progression and sorafenib resistance by inhibiting autophagic degradation of HIF1alpha. J Hepatol 65: 314-324, 2016.
48. Liang XH, Kleeman LK, Jiang HH, Gordon G, Goldman JE, Berry G, Herman B and Levine B: Protection against fatal Sindbis virus encephalitis by beclin, a novel Bcl-2-interacting protein. J Virol 72: 8586-8596, 1998.
49. Guo QQ, Wang SS, Zhang SS, Xu HD, Li XM, Guan Y, Yi F, Zhou TT, Jiang B, Bai N, *et al*: ATM-CHK2-Beclin 1 axis promotes autophagy to maintain ROS homeostasis under oxidative stress. EMBO J 39: e103111, 2020.